

DensePASS: Dense Panoramic Semantic Segmentation via Unsupervised Domain Adaptation with Attention-Augmented Context Exchange

Chaoxiang Ma¹, Jiaming Zhang¹, Kailun Yang¹, Alina Roitberg¹ and Rainer Stiefelhagen¹

Abstract—Intelligent vehicles clearly benefit from the expanded Field of View (FoV) of the 360° sensors, but the vast majority of available semantic segmentation training images are captured with pinhole cameras. In this work, we look at this problem through the lens of domain adaptation and bring *panoramic* semantic segmentation to a setting, where labelled training data originates from a different distribution of conventional *pinhole* camera images. First, we formalize the task of unsupervised domain adaptation for panoramic semantic segmentation, where a network trained on labelled examples from the *source domain* of pinhole camera data is deployed in a different *target domain* of panoramic images, for which no labels are available. To validate this idea, we collect and publicly release DENSEPASS - a novel densely annotated dataset for panoramic segmentation under cross-domain conditions, specifically built to study the PINHOLE→PANORAMIC transfer and accompanied with pinhole camera training examples obtained from Cityscapes. DENSEPASS covers both, labelled- and unlabelled 360° images, with the labelled data comprising 19 classes which explicitly fit the categories available in the source domain (*i.e.* pinhole) data. To meet the challenge of domain shift, we leverage the current progress of attention-based mechanisms and build a generic framework for cross-domain panoramic semantic segmentation based on different variants of attention-augmented domain adaptation modules. Our framework facilitates information exchange at local- and global levels when learning the domain correspondences and improves the domain adaptation performance of two standard segmentation networks by 6.05% and 11.26% in Mean IoU.

I. INTRODUCTION

Semantic segmentation is essential for perception of intelligent vehicles as it enables to locate key entities of a driving scene, such as *road*, *sidewalk* or *person*, by assigning a category label to every image pixel. While semantic segmentation results have increased at a rapid pace since the emergence of fully convolutional networks [1], most of the previous frameworks are developed under the assumption that the images are captured with a *pinhole* camera. However, the comparably narrow Field of View (FoV) largely limits the perception capacity and can be addressed by mounting multiple sensors, which, in return, requires additional mechanisms for data fusion [2]. Recently, leveraging a single *panoramic* camera, which offers a unified 360° perception of the driving

This work was supported in part through the AccessibleMaps project by the Federal Ministry of Labor and Social Affairs (BMAS) under the Grant No. 01KM151112, in part by the University of Excellence through the “KIT Future Fields” project, and in part by Hangzhou SurImage Company Ltd. (Corresponding author: Kailun Yang.)

¹Authors are with Institute for Anthropomatics and Robotics, Karlsruhe Institute of Technology, Germany (e-mail: chaoxiang.ma.1024@gmail.com, {jiaming.zhang, kailun.yang, alina.roitberg, rainer.stiefelhagen}@kit.edu).

Code and dataset will be made publicly available at: <https://github.com/chma1024/DensePASS>

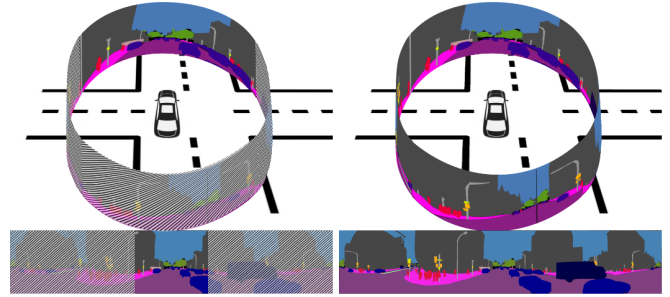


Fig. 1. FoV comparison between pinhole forward-view and 360° panoramic surround-view imaging of self-driving road scenes.

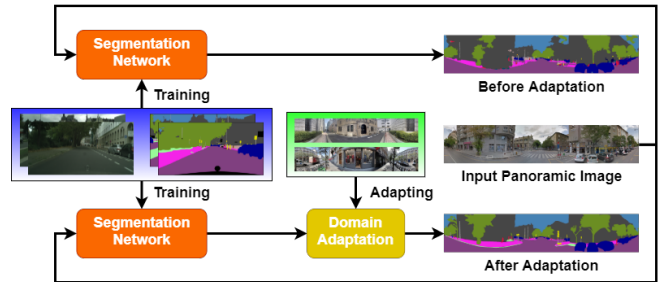


Fig. 2. An overview of the formalized task of domain adaptation for panoramic semantic segmentation. The *source* domain dataset (blue background) contains *pinhole* images with semantic annotations, while the *target* dataset (green background) contains *panoramic* images without annotations.

environment, started to gain attention as a novel alternative for expanding the FoV [3].

Unfortunately, the scarcity of pixel-wise annotation of panoramic images still hinders the progress in the semantic segmentation community. At the same time, *domain adaptation* becomes an increasingly popular research topic, giving a new perspective to complement the insufficient coverage of training data in driving scenarios, *e.g.*, at the nighttime [4] or in accident scenes [5]. In this paper, we argue that panoramic segmentation might strongly benefit from the significantly larger datasets available in the domain of standard image segmentation and explore domain adaptation techniques for such knowledge transfer. Thereby, we formalize the task of unsupervised domain adaptation for panoramic segmentation in a novel Dense PANoramic Semantic Segmentation (DensePASS) benchmark, where images in the label-scarce panoramic *target* domain are handled by adapting from data of the label-rich pinhole *source* domain.

We aim to promote research of *panoramic semantic segmentation under cross-domain conditions* and introduce DensePASS – a new dataset with panoramic images collected all around the globe to encourage diversity. To enable credible quantitative evaluation, our benchmark comprises (1) an unlabelled panoramic training set used for optimization

of the domain adaptation model and (2) a panoramic test set manually labelled with 19 classes defined in accordance to Cityscapes [6], a dataset with pinhole images which we use as training data in the label-rich source domain. Yet, a straightforward transfer of models trained on pinhole images to panoramic data often results in a significant performance drop, since the layout of the panoramic camera images passed through the equirectangular projection strongly differs from the standard pinhole camera data. For example, as shown in Fig. 1, panoramic images have longer horizontal distribution or geometric distortion on both sides of the viewing direction, resulting in a considerable domain shift.

To effectively utilize label-rich pinhole image datasets [6], [7] for label-scarce panoramic segmentation, we systematically examine different Domain Adaptation (DA) strategies for the *Pinhole to Panoramic Domain Adaptation (P2PDA)* (the formalized P2PDA task illustrated in Fig. 2). Furthermore, we implement a P2PDA framework with different DA mechanisms: (i) *Segmentation Domain Adaptation Module (SDAM)*, (ii) *Attentional Domain Adaptation Module (ADAM)*, and (iii) *Regional Context Domain Adaptation Module (RCDAM)*. The proposed *SDAM* module allows greater flexibility than the previous DA methods [8], [9] used in the output space as it can be plugged in at different feature levels. Another challenge is learning good feature representations, which is not only distinguishing various categories with similar appearances, but also linking the same category at diverse locations across the 360° . To address this, we leverage the progress of attention-based models [10], [11], [12] and propose the *ADAM* module for capturing long-range dependencies and positional relations. Lastly, the *RCDAM* module addresses the horizontal distribution of panoramic images and obtains region-level context in order to effectively resist the geometric distortion caused by the equirectangular projection. Extensive experiments demonstrate the effectiveness of our framework, exceeding more than 15 state-of-the-art semantic segmentation methods.

In summary, our main contributions are as following:

- We create and publicly release DensePASS – a new benchmark for panoramic semantic segmentation collected from locations all around the world and densely annotated with 19 classes in accordance to the pinhole camera dataset Cityscapes to enable proper PINHOLE→PANORAMIC evaluation.
- We formalize the problem of unsupervised domain adaptation for panoramic segmentation focused on transfer from label-rich pinhole datasets to DensePASS.
- We propose a generic P2PDA framework and investigate different DA modules both in a separate and joint manner, validating their effectiveness with various networks designed for self-driving scene segmentation.

II. RELATED WORK

A. Semantic Segmentation and Self-attention Modules

The performance of semantic segmentation models has rapidly improved through the explosive rise of deep learning [1], [13], [14], [15]. The first prominent end-to-end

architecture to outperform conventional approaches was the Fully Convolutional Network (FCN) [1] followed by DeepLab [13], PSPNet [14] and DenseASPP [15] leveraging atrous convolutions or pyramid pooling.

At the same time, the use of *self-attention modules* [16], which learn to automatically weigh input positions (*i.e.* temporal [16] or spatial [10]), increasingly gains interest in the field. Such mechanisms are widely used for capturing long-range contextual dependencies which are crucial for dense prediction tasks. The success of attention mechanisms in visual recognition [10], leads to their explorations in some semantic segmentation works focused on both, accuracy-oriented networks [11], [17], [18] and efficiency-oriented networks [12], [19], [20]. For example, FANet [12] proposed a fast self-attention module for non-local context aggregation aiming efficient segmentation, whereas DANet [11] was designed with position and channel attention modules to learn spatial and channel interdependencies.

We leverage such attention principles to mitigate the domain shift by highlighting regional context and present a cross-domain segmentation framework with *attentional domain adaptation modules*. We experiment with both, accuracy- and efficient-oriented networks [11], [12], [21] as the segmentation architecture, and demonstrate the consistent effectiveness of our adaptation modules for bringing standard semantic segmentation model to panoramic imagery.

B. Semantic Segmentation for Panoramic Images

Segmentation of panoramic data, which is often captured through distortion-heavy fisheye lenses [22], [23] or multiple cameras [2], [24], is especially challenging as it requires eliminating distortions, synchronizing and calibrating the cameras, and fusing the data, which leads to higher latency. Yang *et al.* introduced the PASS [3] and the DS-PASS [25] frameworks which successfully mitigate the effect of distortions by using a panoramic annular lens system but come with a high memory- and computational cost. This was significantly improved by the OOSS framework [26] through multi-source omni-supervised learning for omnidirectional segmentation. The latest advancements include frameworks focusing on omni-range contextual dependencies [19] or leveraging pixel-level contrastive pre-training [27].

All previous frameworks [3], [19], [27] are developed under the assumption that the labelled training data are implicitly or partially available in our target domain of panoramic images. Since panoramic datasets are comparably small in size, we argue, that *panoramic* segmentation might strongly benefit from the significantly larger datasets available in the domain of *standard* image segmentation. To achieve this, we look at panoramic segmentation from a *domain adaptation perspective* and introduce the DensePASS dataset covering images with 19 annotated categories in both, standard- and panoramic domains. We further introduce a framework for unsupervised domain adaptation for panoramic semantic segmentation, where we combine prominent segmentation approaches with attention-based adaptation modules.

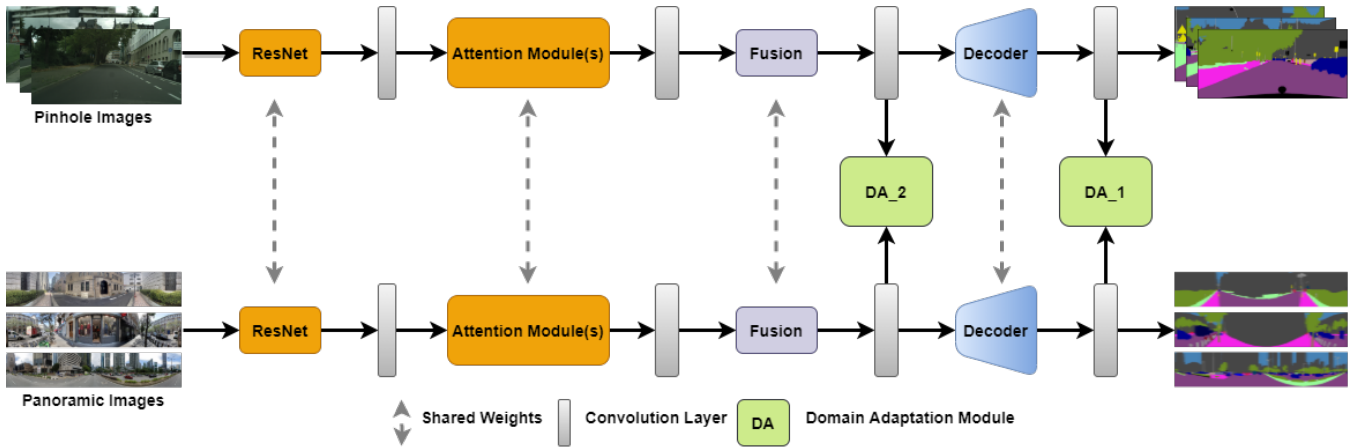


Fig. 3. An overview of the proposed P2PDA framework. Our main backbone is a segmentation network with attention modules. DA_2 and DA_1 are different domain adaptation modules we use in multi-levels. Images from pinhole source domain and panoramic target domain will be fed into the segmentation network to generate semantic segmentation predictions. Fusion layers fuse the attended feature maps after the attention modules. Meanwhile, feature maps from the last layer and before the decoder will be inputted into DA_1 and DA_2, respectively, to adapt from the pinhole source domain to the panoramic target domain. SDAM can be used in both DA_1 and DA_2, ADAM can be used in DA_2 and RCDAM can be used in DA_1.

C. Domain Adaptation for Semantic Segmentation

Domain adaptation has been recently addressed in the *standard* semantic segmentation, by either (1) optimizing the *source* domain networks on pseudo-labels generated by a model trained in the *source* domain [28], [29], or (2) leveraging a Generative Adversarial Network (GAN) [30] to learn domain translations [4], [8], [9], [31]. To utilize the significant amount of *source-target* similarities in the resulting segmentation masks, Tsai *et al.* [8] aligned the domains in output space via adversarial learning (AdaptSegNet). Chang *et al.* [9] introduced the DISE framework which extracts domain-invariant structure and domain-specific texture information to reduce the source-target discrepancies. Attention mechanisms also started gaining attention for domain adaptation with techniques such as attentional transfer [32] or multiple cross-domain attention modules for obtaining context dependencies from both local and global perspectives [33].

We specifically focus on domain transfer for *panoramic* semantic segmentation, which differs from the *standard pinhole* images in several important aspects, such as discontinuous boundaries and distorted objects. To capture long-range correlations between pixels and semantic regions, we extend AdaptSegNet [8] with attention-augmented modules in multiple stages and a regional context exchange, leading to a significant adaptation improvement.

III. P2PDA: PROPOSED FRAMEWORK

In this work, we introduce a generic framework for 360° perception of self-driving scenes by learning to adapt semantic segmentation networks from a label-rich source domain of standard pinhole camera images to the unlabelled target domain of panoramic data. Conceptually, our framework comprises encoder-decoder-based semantic segmentation network and three different building blocks for domain alignment: Segmentation domain adaptation module (SDAM), Attentional domain adaptation module (ADAM) and Regional context domain adaptation module (RCDAM), which we place at two different network stages: after and

before the decoder of the segmentation network (denoted as DA_2 and DA_1 respectively). Next, we present an overview of the proposed framework (Sec. III-A) and describe the three integrated domain adaptation modules in detail (Sec. III-B).

A. Framework Overview

Our framework builds on the AdaptSegNet model [8], extending it with multiple versions of region- or attention-augmented DA modules placed at different network levels with an overview provided in Fig. 3. The main components of our framework are a weight-shared segmentation network \mathbf{G} with attention modules and two DA modules (DA_2 and DA_1) with corresponding discriminators \mathbf{D} . We denote the source domain images as I_s and target domain images as I_t . For simplicity, I_s and I_t also refer to the intermediate feature map representations of the images.

At first, the source domain images I_s are fed into the segmentation network \mathbf{G} (also referred to as the generator) to generate prediction results and the source ground-truth labels are used to compute the segmentation loss \mathcal{L}_{seg} . Next, the corresponding feature maps are passed to the domain adaptation modules in order to close the gap between the source and target domains at different network levels. The discriminators are trained with the binary objective to estimate the domain of the input data, so that the discriminator loss $\mathcal{L}_D(I_s, I_t)$ is a cross-entropy loss with two classes (panoramic and pinhole). The discriminator output of the target domain data I_t is directly used to estimate the adversarial loss $\mathcal{L}_{adv}[\mathbf{D}(I_t)]$ for the generator training (alongside with \mathcal{L}_{seg}) and is high if the discriminator prediction is correct (so the adversarial loss facilitates generation of segmentation masks in the target domain which successfully “fool” the discriminator). In other words, the discriminators are trained to distinguish between the source and target domains with $\mathcal{L}_D(I_s, I_t)$, while the segmentation network \mathbf{G} is trained to 1) correctly segment the images from the source domain with \mathcal{L}_{seg} , and 2) “fool” the discriminator by making the target domain data indistinguishable from the source domain data. The final loss

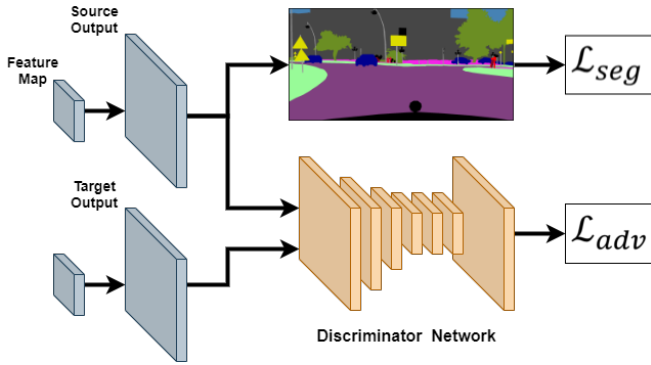


Fig. 4. An overview of the SDAM module.

used to train the generator becomes:

$$\mathcal{L}_G(I_s, I_t) = \lambda_{seg} \mathcal{L}_{seg}(I_s) + \lambda_{adv} \mathcal{L}_{adv}[\mathbf{D}(I_t)],$$

where λ_{adv} and λ_{seg} are weights used to balance the domain adaptation and semantic segmentation losses.

B. Domain Adaptation Modules

We now explain the three integrated DA modules in detail. **Segmentation domain adaptation module (SDAM).** Our initial domain adaptation module SDAM is derived from AdaptSegNet and attempts to align the segmentation output of the source and target maps (the module is illustrated in Fig. 4). After a segmentation network forward pass with both, an image from the source and target domains (I_s and I_t), feature maps of the both representations are used as input to the discriminator \mathbf{D} which learns to predict the domain with $\mathcal{L}_D(I_s, I_t)$, while the segmentation network G learns to correctly segment the pinhole images with $\mathcal{L}_{seg}(I_s)$ and align the domains with $\mathcal{L}_{adv}[\mathbf{D}(I_t)]$. The SDAM learns a PINHOLE→PANORAMIC domain adaptation model at *multiple levels jointly* (i.e. integration in DA_1 and DA_2).

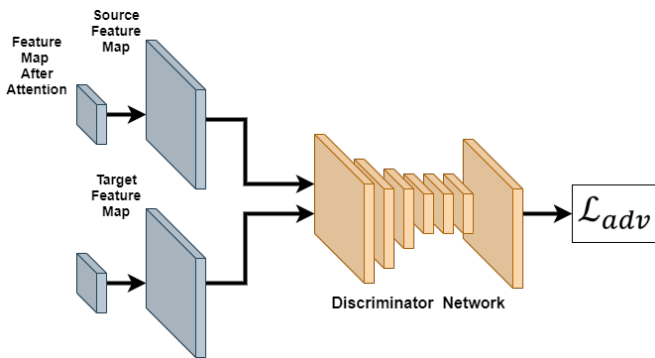


Fig. 5. An overview of the ADAM module.

Attentional domain adaptation module (ADAM). To detect and effectively utilize the significant amount of pinhole-panoramic correspondences at both, local and global scale, we design *ADAM*, an *attentional* domain adaptation module (overview in Fig. 5). ADAM differs from SDAM as it leverages the attention mechanism to learn an optimal weighting scheme for the features used as the discriminator input. By doing this, ADAM enables direct information exchange among all pixels, mitigating the influence of discrepancy in

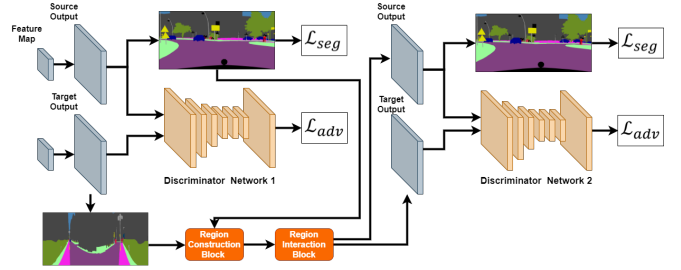


Fig. 6. An overview of the RCDAM module.

positional priors and local distortions. Relevant portions of the feature maps of both, I_s and I_t inputs are magnified through the attention and the *re-weighted* source and target representations are both used to optimize the corresponding discriminator \mathbf{D} with adversarial loss. Since ADAM operates on attended feature maps with long-range contextual dependency aggregation, it is used in DA_2 only.

Regional context domain adaptation module (RCDAM). Next, we focus on *region relationship of the panoramic images*. Inspired by RANet [17], we design the RCDAM module to configure the information flow between different regions and within the same region, as illustrated in Fig. 6.

RCDAM follows a hierarchical adversarial learning scheme with two-stage discriminators, where the first stage is identical to the previously described SDAM. The second stage covers two blocks: a Region Construction Block (RCB) and a Region Interaction Block (RIB) first introduced in RANet. The inputs to this stage are the feature maps of I_s and I_t after a segmentation network forward pass.

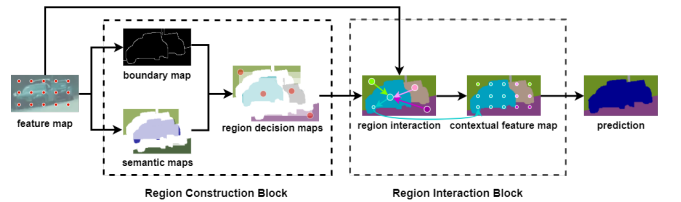


Fig. 7. Diagram of Region Construction and Region Interaction Blocks.

Fig. 7 gives a detailed overview of the RCB and RIB building blocks. RCB computes a boundary map and semantic maps as in [17] to link each pixel (the red dot in Fig. 7) to different semantic regions. Then, RCB conducts a region decision map with the representative pixels (the larger dots). After that, RIB selects representative pixels (the larger dots in color) for each region and summarizes information from the pixels (the smaller dots) in the same region into representative pixels. Next, RIB aggregates the information from representative pixels in other regions to form the global contextual representations which are afterwards propagated to all pixels in the image. At last, regional context is sufficiently exchanged and new regional context-driven feature maps are built to generate final prediction outputs, which will be used to perform the same operations as in the first stage. It is worth noting that, the second stage is used to help improve the segmentation result in the first stage, which can make the result more compact and helps the adaptation between the pinhole domain and the panoramic domain by exchanging

TABLE I. Per-class results on DensePASS. We use FANet [12] as the segmentation network and set different domain adaptation modules for DA_2 and DA_1 to test our methods on DensePASS with the size of input 2048×400 . S represents the segmentation domain adaptation module, A represents the attentional domain adaptation module and S+A represents a combination of S and A. The first line is the Cityscapes source-only result without adaptation.

| Methods | DA_2 | DA_1 | Mean IoU | road | sidewalk | building | wall | fence | pole | traffic light | traffic sign | vegetation | terrain | sky | person | rider | car | truck | bus | train | motorcycle | bicycle |
|---------|------|------|--------------|--------------|--------------|--------------|--------------|--------------|--------------|---------------|--------------|--------------|--------------|--------------|--------------|--------------|--------------|--------------|-------------|--------------|--------------|--------------|
| FANet | - | - | 26.90 | 62.98 | 10.64 | 72.41 | 7.80 | 20.74 | 11.77 | 6.85 | 3.75 | 68.11 | 21.56 | 87.00 | 23.73 | 5.33 | 49.61 | 10.65 | 0.54 | 16.76 | 24.15 | 6.62 |
| FANet | S | S | 32.17 | 62.16 | 16.85 | 78.78 | 13.67 | 24.07 | 19.72 | 11.42 | 9.68 | 71.42 | 18.22 | 85.72 | 32.66 | 11.75 | 54.34 | 17.61 | 0.00 | 41.52 | 29.30 | 12.30 |
| FANet | A | S | 32.67 | 62.28 | 16.86 | 79.99 | 17.64 | 23.96 | 19.78 | 12.33 | 9.58 | 72.01 | 19.29 | 85.91 | 32.85 | 11.03 | 55.75 | 15.38 | 0.38 | 43.53 | 29.19 | 12.95 |
| FANet | S+A | S | 33.05 | 61.74 | 17.70 | 80.07 | 16.38 | 24.64 | 19.61 | 12.04 | 9.79 | 72.27 | 17.94 | 86.31 | 33.17 | 11.47 | 55.18 | 15.61 | 0.04 | 52.55 | 28.68 | 12.82 |

regional context. Thereby, the final output is from the first stage, which means this domain adaptation module does not change the original architecture of the segmentation network and can be used for networks without attention layers.

IV. NEW BENCHMARK AND EXPERIMENTS

To evaluate the idea of panoramic segmentation through domain adaptation from standard pinhole camera images, we conduct extensive experiments with different variants of our P2PDA framework. First, we introduce the novel DensePASS dataset for dense *panoramic* segmentation of driving scenes annotated in accordance to the *pinhole* camera dataset Cityscapes (Sec. IV-A). Then, we quantitatively validate how well the P2PDA framework can handle the PINHOLE→PANORAMIC transfer and conduct extensive ablation studies for different versions of DA modules and two segmentation networks: the speed-oriented FANet [12] (Sec. IV-B) and accuracy-oriented DANet [11] (Sec. IV-C). We further benchmark our framework against more than 15 state-of-the-art segmentation models (Sec. IV-D) and examine the impact of expanding the training data with another source dataset (Sec. IV-E). Finally, we showcase multiple qualitative examples of the achieved results (Sec. IV-F). We adopt Mean Intersection over Union (IoU) as our main evaluation metric.

A. Dataset and Experimental Settings

Source dataset (pinhole). We use Cityscapes [6] as our label-rich source dataset providing a large amount of annotated pinhole camera images. Cityscapes covers 2979 training- and 500 validation examples captured in 50 different European cities and annotated with 19 categories. We use the 2979 training samples as our source training data.

DensePASS target dataset (panoramic). Since no established segmentation benchmarks target the PINHOLE→PANORAMIC transfer and previous panoramic test-beds cover a very small number of classes [3][19], we collect DensePASS – a novel densely annotated dataset for panoramic segmentation of driving scenes. While DensePASS could also be used for the the same-domain panormaic segmentation, it is specifically built with the PINHOLE→PANORAMIC transfer in mind, so that the test data is annotated with 19 categories present in the pinhole camera dataset Cityscapes. To facilitate the unsupervised domain adaptation task, DensePASS covers both, labelled data (100 panoramic images used for testing) and unlabelled training data (2000 panoramic images used for the domain transfer optimization). Panoramic images (2048×400

resolution) are collected using Google Street View, spanning images from different continents (25 different cities for testing and 40 for training).

Training settings. We use stochastic gradient descent (initial learning rate of $1e-5$, momentum of 0.9 and a decay of $5e-4$) for optimization of the segmentation network **G** and the Adam optimizer for discriminators **D** (initial learning rate set to $4e-6$). For both optimizers, the learning rate is decreased polynomially where the learning rate is multiplied by $(1 - \frac{iter}{max_iter})^{0.9}$ after each iteration, where max_iter is set to 200000 with a batch-size of 2. The loss balancing weights, λ_{adv} and λ_{seg} are set to 0.001 and 1.0 for DA_1, and 0.0002 and 0.1 for DA_2. In the RCDAM module, λ_{seg} is set to 1.5 for the prediction result before RCB. During training, pinhole images are resized to 1280×720 while panoramic data is kept at the 2048×400 resolution.

B. Ablation Studies for Segmentation Network with FANet

We first consider FANet [12], a lightweight speed-oriented network, as the segmentation model and investigate different combinations of domain adaptation modules for DA_2 and DA_1. As shown in Table I, before adaptation, FANet yields a mean IoU of 26.90% indicating large room for improvement in cross-domain generalization. Our framework improves the result to 32.17% by using the SDAM module in both DA_2 and DA_1 (5.27% gain). Integrating the attentional ADAM module also leads to a considerable boost (32.67% IOU, a 5.77% gain over the the source-only baseline). A combination of the SDAM and ADAM modules in DA_2 yields the best recognition result of 33.05% IoU.

C. Ablation Studies for Segmentation Network with DANet

Next, we experiment with a heavier and more accuracy-oriented segmentation network DANet [11] (results provided in Table II). The native source-trained DANet achieves a mean IoU of only 28.50%, highlighting the sensitivity of modern segmentation networks to the PINHOLE→PANORAMIC domain shift. The performance is strongly improved (10.01% boost) through SDAM modules placed in DA_2 and DA_1, achieving 38.51% in mean IoU. Similarly, using the ADAM module in DA_2 yields a result of 39.16% (a 10.66% improvement over the source-only baseline). Combining both the SDAM and ADAM modules again slightly improves the performance (39.28% mean IoU).

We further explore the use of the RCDAM module in DA_1, yielding 39.46% mIoU (10.96% boost over the baseline). The best performance of 39.76% (11.26% boost with

TABLE II. Per-class results on DensePASS. We use DANet [11] as the segmentation network and set different domain adaptation modules for DA_2 and DA_1 to test our methods on DensePASS with the size of input 2048×400 . S represents the segmentation domain adaptation module, A represents the attentional domain adaptation module, R represents the regional context domain adaptation module and S+A represents a combination of S and A. The first line is the Cityscapes source-only result without adaptation. * denotes further adding source images from WildDash to complement Cityscapes.

| Methods | DA_2 | DA_1 | Mean IoU | road | sidewalk | building | wall | fence | pole | traffic light | traffic sign | vegetation | terrain | sky | person | rider | car | truck | bus | train | motorcycle | bicycle |
|---------|------|------|--------------|--------------|--------------|--------------|--------------|--------------|--------------|---------------|--------------|--------------|--------------|--------------|--------------|--------------|--------------|--------------|--------------|--------------|--------------|--------------|
| DANet | - | - | 28.50 | 70.68 | 8.30 | 75.80 | 9.49 | 21.64 | 15.91 | 5.85 | 9.26 | 71.08 | 31.50 | 85.13 | 6.55 | 1.68 | 55.48 | 24.91 | 30.22 | 0.52 | 0.53 | 17.00 |
| DANet | S | S | 38.51 | 61.78 | 21.11 | 74.59 | 22.59 | 29.93 | 14.79 | 15.00 | 10.17 | 66.94 | 19.03 | 82.57 | 31.03 | 21.24 | 53.26 | 54.67 | 37.77 | 39.40 | 43.84 | 31.95 |
| DANet | A | S | 39.16 | 61.34 | 20.71 | 76.52 | 20.53 | 30.03 | 14.19 | 15.69 | 10.09 | 68.60 | 18.84 | 82.08 | 33.16 | 21.75 | 57.68 | 53.88 | 40.33 | 41.47 | 46.11 | 31.00 |
| DANet | S+A | S | 39.28 | 62.43 | 21.89 | 76.22 | 21.42 | 30.54 | 14.85 | 14.10 | 9.76 | 69.07 | 19.94 | 82.84 | 34.56 | 19.30 | 56.51 | 53.04 | 42.51 | 39.47 | 45.71 | 32.09 |
| DANet | S | R | 39.46 | 62.75 | 23.17 | 76.65 | 23.90 | 30.82 | 14.84 | 18.44 | 10.09 | 69.10 | 17.60 | 82.78 | 33.51 | 21.53 | 55.97 | 51.78 | 41.77 | 36.90 | 46.11 | 32.12 |
| DANet | S+A | R | 39.76 | 63.11 | 24.63 | 76.17 | 25.03 | 30.56 | 13.68 | 15.68 | 10.53 | 67.31 | 22.41 | 80.15 | 32.95 | 21.11 | 54.39 | 53.51 | 43.64 | 42.20 | 46.71 | 31.66 |
| DANet* | S | R | 41.35 | 68.38 | 37.26 | 75.51 | 26.28 | 31.81 | 15.62 | 8.99 | 10.33 | 66.22 | 31.74 | 80.68 | 33.69 | 16.81 | 64.81 | 47.67 | 28.05 | 61.81 | 44.92 | 34.98 |
| DANet* | S+A | R | 42.47 | 67.47 | 30.16 | 75.27 | 30.26 | 37.50 | 16.19 | 9.35 | 9.78 | 63.14 | 30.44 | 77.07 | 34.82 | 15.24 | 64.33 | 53.70 | 43.33 | 71.57 | 46.80 | 30.47 |

TABLE III. Performance of models on Cityscapes and DensePASS.

| Network | Backbone | Cityscapes | DensePASS | mIoU Gap |
|---------------------|---------------|------------|-----------|----------|
| DeepLabV3+ [13] | ResNet-18 | 76.8 | 25.6 | -51.2 |
| OCRNet [18] | HRNetV2p-W18s | 77.1 | 25.9 | -51.2 |
| Fast-SCNN [34] | Fast-SCNN | 69.1 | 24.6 | -44.5 |
| DeepLabV3+ [13] | ResNet-50 | 80.1 | 29.0 | -51.1 |
| PSPNet [14] | ResNet-50 | 78.6 | 29.5 | -49.1 |
| DNL [35] | ResNet-50 | 79.3 | 28.7 | -50.6 |
| Semantic FPN [36] | ResNet-50 | 74.5 | 29.9 | -44.6 |
| OCRNet [18] | HRNetV2p-W18 | 78.6 | 30.8 | -47.8 |
| DeepLabV3+ [13] | ResNet-101 | 80.9 | 32.5 | -48.4 |
| PSPNet [14] | ResNet-101 | 79.8 | 30.4 | -49.4 |
| DNL [35] | ResNet-101 | 80.4 | 32.1 | -48.3 |
| Semantic FPN [36] | ResNet-101 | 75.8 | 28.8 | -47.0 |
| ResNeSt [37] | ResNeSt-101 | 79.6 | 28.8 | -50.8 |
| OCRNet [18] | HRNetV2p-W48 | 80.7 | 32.8 | -47.9 |
| ERFNet [21] | ERFNet | 72.1 | 16.7 | -55.4 |
| ERFNet-P2PDA (Ours) | ERFNet | 72.1 | 34.1 | -38.0 |
| FANet [12] | ResNet-34 | 71.3 | 26.9 | -44.4 |
| FANet-P2PDA (Ours) | ResNet-34 | 71.3 | 33.1 | -38.2 |
| DANet [11] | ResNet-50 | 79.3 | 28.5 | -50.8 |
| DANet-P2PDA (Ours) | ResNet-50 | 79.3 | 39.8 | -39.5 |

respect to the original segmentation network) is achieved by combining all three modules: SDAM and ADAM in DA_2 and RCDAM in DA_1. Overall, our experiments showcase that direct cross-domain semantic segmentation is a hard task and P2PDA framework with attentional and regional domain adaptation modules clearly helps to close the domain gap.

D. Benchmarking and Comparison with the State-of-the-Art

Our previous experiments compared different P2PDA framework configurations with each other and the native segmentation network. Next, we aim to quantify the domain gap between the pinhole- and panoramic images and extend our evaluation with over 15 off-the-shelf segmentation models trained on Cityscapes and evaluated on both, Cityscapes (no domain shift) and the panoramic DensePASS images.¹ Table III summarizes our results. It is evident, that modern segmentation models trained on pinhole camera images struggle with generalization to panoramic data, with performance degrading by $\sim 50\%$ as we move from the standard PINHOLE \rightarrow PINHOLE setting to the PINHOLE \rightarrow PANORAMIC evaluation. We also verify our P2PDA domain adaptation strategy with three different

¹For a fair comparison, model weights are provided by the same framework MMSegmentation: <https://github.com/open-mmlab/mms Segmentation>

segmentation models (bottom part of Table III). Our P2PDA strategy with regional and attentional context exchange improves the PINHOLE \rightarrow PANORAMIC results by a large margin (mIoU gains of 17.4%, 6.2% and 11.3% for ERFNet, FANet and DANet, respectively). Our experiments provide encouraging evidence that P2PDA can be successfully deployed for cross-domain 360 $^\circ$ understanding of driving scenes.

E. Complementing the Cityscapes Source with WildDash

Our next area of investigation is the impact of expanding the source data with a more complex dataset, since DensePASS contains highly composite scenes due to larger FoV, while Cityscapes is large but relatively simple. To achieve this, we leverage the WildDash dataset [7] with 4256 pinhole images, pixel-level annotations and more unstructured surroundings. As shown in the last two rows of Table II, we obtain better mIoU with the expanded training set, achieving 41.35% and 42.47% with different P2PDA variants. Interestingly, the IoUs of *road*, *sidewalk*, *terrain*, *car*, and *train* are significantly improved, which we link to the strong positional priors of these categories in structured urban scenes, while DensePASS and WildDash environment is more chaotic and unconstrained. Furthermore, direct comparison of the two P2PDA versions demonstrates the effectiveness of the attention-augmented adaptation strategy.

F. Qualitative Analysis

In our final study, we showcase multiple examples of representative qualitative results in Fig. 8. The segmentation boundaries of regions such as *sky*, *building*, and *vegetation* are clearly improved through the P2PDA strategy in every case, while *sidewalk* segmentation clearly benefits from domain adaptation in the second row example. At the same time, some misclassified categories are corrected after adaptation (e.g., *car* and *truck* in all examples). There is also more clarity as it comes to detailed segmentation of small objects, such as *traffic light* and *traffic sign* in the first and the second row, as well as *pole* in all rows. These qualitative examples consistently confirm the conclusions of our quantitative evaluation, highlighting the benefits of the proposed P2PDA strategy for 360 $^\circ$ self-driving scene understanding through domain adaptation from pinhole camera data.

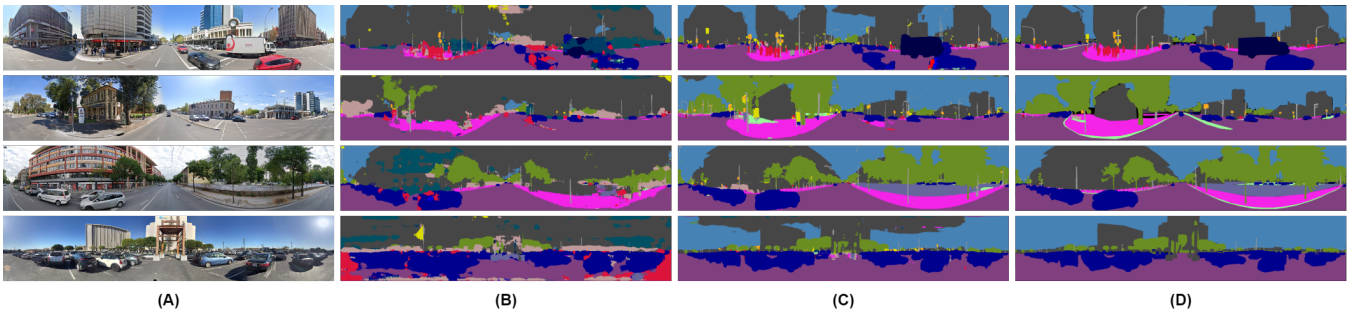


Fig. 8. Qualitative examples of semantic segmentation on 360° panoramic images. For each row, (A) is the original input panoramic image, (B) is the segmentation result without any adaptation, (C) is the segmentation result with our proposed P2PDA adaptation framework, and (D) is the ground truth.

V. CONCLUSION

Semantic scene understanding is vital for autonomous driving but requires models which can deal with changes in data distribution. In this work, we introduced the new task of cross-domain semantic segmentation for panoramic driving scenes, which extends the standard panoramic segmentation with the premise of the training data originating from a different domain (e.g. pinhole camera images). First, we formulate the problem of unsupervised domain adaptation for panoramic segmentation and introduce the novel DensePASS dataset which we use to study the PINHOLE→PANORAMIC transfer. To meet the challenge of domain divergence, we developed a generic framework enhancing conventional segmentation algorithms with different domain adaptation modules. While our experiments demonstrate that cross-domain panoramic segmentation task is difficult for modern algorithms, our proposed domain-agnostic framework with attention-based domain adaptation modules consistently improves the results. Our dataset will be publicly released upon publication and we believe that DensePASS has strong potential to motivate the needed development of *generalizable* semantic segmentation models.

REFERENCES

- [1] J. Long, E. Shelhamer, and T. Darrell, “Fully convolutional networks for semantic segmentation,” in *IEEE CVPR*, 2015.
- [2] L. Deng, M. Yang, H. Li, T. Li, B. Hu, and C. Wang, “Restricted deformable convolution-based road scene semantic segmentation using surround view cameras,” *IEEE Trans. Intell. Transp. Syst.*, 2020.
- [3] K. Yang, X. Hu, L. M. Bergasa, E. Romera, and K. Wang, “PASS: Panoramic annular semantic segmentation,” *IEEE Trans. Intell. Transp. Syst.*, 2020.
- [4] E. Romera, L. M. Bergasa, K. Yang, J. M. Alvarez, and R. Barea, “Bridging the day and night domain gap for semantic segmentation,” in *IEEE Intell. Vehicles Symp. (IV)*, 2019.
- [5] J. Zhang, K. Yang, and R. Stiefelhagen, “ISSAFE: Improving semantic segmentation in accidents by fusing event-based data,” *CoRR*, 2020.
- [6] M. Cordts *et al.*, “The cityscapes dataset for semantic urban scene understanding,” in *IEEE Conf. Comput. Vis. Pattern Recognit.*, 2016.
- [7] O. Zendel, K. Honauer, M. Murschitz, D. Steininger, and G. F. Dominguez, “WildDash - Creating hazard-aware benchmarks,” in *Eur. Conf. Comput. Vis.*, 2018.
- [8] Y. Tsai, W. Hung, S. Schulter, K. Sohn, M. Yang, and M. Chandraker, “Learning to adapt structured output space for semantic segmentation,” in *IEEE/CVF Conf. Comput. Vis. Pattern Recognit. (CVPR)*, 2018.
- [9] W. Chang, H. Wang, W. Peng, and W. Chiu, “All about structure: Adapting structural information across domains for boosting semantic segmentation,” in *IEEE Conf. Comput. Vis. Pattern Recognit.*, 2019.
- [10] X. Wang, R. B. Girshick, A. Gupta, and K. He, “Non-local neural networks,” in *IEEE Conf. Comput. Vis. Pattern Recognit.*, 2018.
- [11] J. Fu *et al.*, “Dual attention network for scene segmentation,” in *IEEE/CVF Conf. Comput. Vis. Pattern Recognit. (CVPR)*, 2019.
- [12] P. Hu *et al.*, “Real-time semantic segmentation with fast attention,” *IEEE Robotics Autom. Lett.*, 2021.
- [13] L. Chen, Y. Zhu, G. Papandreou, F. Schroff, and H. Adam, “Encoder-decoder with atrous separable convolution for semantic image segmentation,” in *Eur. Conf. Comput. Vis.*, 2018.
- [14] H. Zhao, J. Shi, X. Qi, X. Wang, and J. Jia, “Pyramid scene parsing network,” in *IEEE Conf. Comput. Vis. Pattern Recognit. (CVPR)*, 2017.
- [15] M. Yang, K. Yu, C. Zhang, Z. Li, and K. Yang, “DenseASPP for semantic segmentation in street scenes,” in *IEEE CVPR*, 2018.
- [16] A. Vaswani *et al.*, “Attention is all you need,” in *NeurIPS*, 2017.
- [17] D. Shen, Y. Ji, P. Li, Y. Wang, and D. Lin, “RANet: Region attention network for semantic segmentation,” *NeurIPS*, 2020.
- [18] Y. Yuan, X. Chen, and J. Wang, “Object-contextual representations for semantic segmentation,” in *Eur. Conf. Comput. Vis.*, 2020.
- [19] K. Yang, J. Zhang, S. Reiß, X. Hu, and R. Stiefelhagen, “Capturing omni-range context for omnidirectional segmentation,” in *IEEE/CVF Conf. Comput. Vis. Pattern Recognit. (CVPR)*, 2021.
- [20] Q. Song, K. Mei, and R. Huang, “Attention-Augmented network for fast and accurate scene parsing,” in *AAAI*, 2021.
- [21] E. Romera, J. M. Alvarez, L. M. Bergasa, and R. Arroyo, “ERFNet: Efficient residual factorized ConvNet for real-time semantic segmentation,” *IEEE Trans. Intell. Transp. Syst.*, 2018.
- [22] Y. Ye, K. Yang, K. Xiang, J. Wang, and K. Wang, “Universal semantic segmentation for fisheye urban driving images,” in *IEEE SMC*, 2020.
- [23] C. Playout, O. Ahmad, F. Lécué, and F. Chériet, “Adaptable deformable convolutions for semantic segmentation of fisheye images in autonomous driving systems,” *CoRR*, 2021.
- [24] V. Ravikumar *et al.*, “OmniDet: Surround view cameras based multi-task visual perception network for autonomous driving,” *IEEE Robotics Autom. Lett.*, 2021.
- [25] K. Yang, X. Hu, H. Chen, K. Xiang, K. Wang, and R. Stiefelhagen, “DS-PASS: Detail-sensitive panoramic annular semantic segmentation through swafnet for surrounding sensing,” in *IEEE IV*, 2020.
- [26] K. Yang, X. Hu, Y. Fang, K. Wang, and R. Stiefelhagen, “Omnisupervised omnidirectional semantic segmentation,” *IEEE T-ITS*, 2020.
- [27] A. Jaus, K. Yang, and R. Stiefelhagen, “Panoramic panoptic segmentation: Towards complete surrounding understanding via unsupervised contrastive learning,” in *IEEE Intell. Vehicles Symp. (IV)*, 2021.
- [28] Q. Lian, L. Duan, F. Lv, and B. Gong, “Constructing self-motivated pyramid curriculums for cross-domain semantic segmentation: A non-adversarial approach,” in *IEEE Int. Conf. Comput. Vis.*, 2019.
- [29] Y. Zou, Z. Yu, X. Liu, B. V. K. V. Kumar, and J. Wang, “Confidence regularized self-training,” in *IEEE Int. Conf. Comput. Vis.*, 2019.
- [30] I. J. Goodfellow *et al.*, “Generative adversarial nets,” in *NeurIPS*, 2015.
- [31] J. Hoffman, D. Wang, F. Yu, and T. Darrell, “FCNs in the wild: Pixel-level adversarial and constraint-based adaptation,” *CoRR*, 2016.
- [32] D. Kothandaraman, R. Chandra, and D. Manocha, “SAfE: Self-Attention based unsupervised road safety classification in hazardous environments,” *CoRR*, 2020.
- [33] J. Yang, W. An, C. Yan, P. Zhao, and J. Huang, “Context-aware domain adaptation in semantic segmentation,” in *IEEE WACV*, 2021.
- [34] R. P. K. Poudel, S. Liwicki, and R. Cipolla, “Fast-SCNN: Fast semantic segmentation network,” in *Brit. Mach. Vis. Conf.*, 2019.
- [35] M. Yin *et al.*, “Disentangled non-local neural networks,” in *Eur. Conf. Comput. Vis.*, 2020.
- [36] A. Kirillov, R. Girshick, K. He, and P. Dollár, “Panoptic feature pyramid networks,” in *IEEE CVPR*, 2019.
- [37] H. Zhang *et al.*, “ResNeSt: Split-Attention networks,” *CoRR*, 2020.